

MHD FLOW AND HEAT TRANSFER OF A MICROPOLAR FLUID OVER A STRETCHABLE DISK

MUHAMMAD ASHRAF, KIRAN BATOOL

*Bahauddin Zakariya University, Centre for Advanced Studies in Pure and Applied Mathematics, Multan, Pakistan
e-mail: mashraf_mul@yahoo.com*

A numerical study of an axisymmetric steady laminar incompressible flow of an electrically conducting micropolar fluid over a stretchable disk is carried out when the fluid is subjected to an external transverse magnetic field. The governing nonlinear equations of motion are transformed into a dimensionless form through Von Karman's logic similarity functions. An algorithm based on a finite difference scheme is used to solve the reduced coupled nonlinear ordinary differential equations with the associated boundary conditions. Effects of the micropolar parameters, the magnetic parameter and the Prandtl number on the flow velocity and temperature distribution are discussed. Investigations predict that the heat transfer rate at the surface of the disk increases with an increase in the values of micropolar parameters. The magnetic field enhances the shear and couple stresses. The shear stress factor is lower for micropolar fluids as compared to Newtonian fluids, which may be beneficial in flow and heat control of polymeric processing.

Key words: magnetohydrodynamics (MHD), micropolar fluids, heat transfer, stretchable disk

1. Introduction

The study of flow and heat transfer over a stretching surface has generated much interest in recent years in view of its numerous industrial applications such as extrusion of polymer sheets, extrusion of plastic sheet, rolling and manufacturing plastic films, artificial fibres, extrusion paper production, glass blowing, metal spinning, metal industries and drawing plastic films. The rate of heat transfer at the stretching surface determines the quality of the final product. The flow of an incompressible viscous fluid over a stretching surface has an important bearing on several technological applications in the field of metallurgy and chemical engineering.

Nature is abundant with examples of flows involving non-Newtonian fluids. The flow of non-Newtonian fluids occurs in a wide variety of applications: from oil and gas well drilling, to well completion operations, from industrial processes involving waste fluids, synthetic fibres, foodstuffs to extrusion of molten plastic, and as well as in some flows of polymer solutions. This class of fluids represents mathematically many industrially important fluids, as paints, blood, body fluids, polymers, colloidal fluids and suspension fluid and is expected to provide a mathematical model for the non-Newtonian fluid behavior. Such flows have been attracting the attention of investigators for a long time. This attraction has been considerably growing especially during the last few decades. The resulting equations of non-Newtonian fluids are nonlinear, high order, and much more complicated than the Navier Stokes (NS) equation. The flow characteristics of non-Newtonian fluids are quite different in comparison to Newtonian fluids.

The theory of micropolar fluids introduced by Eringen (1964, 1966) takes into account the microscopic effect arising from the local microstructure and intrinsic motion of fluid particles, and is expected to provide a mathematical model for the non-Newtonian fluid behavior. Such fluids can be subjected to surface and body couples in which the material points in a volume element

can undergo motions about the centre of masses along with the deformation. In practice, the theory requires that one must solve an additional transport equation representing the principle of conservation of local angular momentum as well as the usual transport equation for the conservation of mass and linear momentum, and additional constitutive parameters are also introduced.

The surface stretching problem was first proposed and analyzed by Sakiadis (1961) based on the boundary layer approximation. Crane (1970) presented an exact solution of the two dimensional NS equations for a stretching sheet problem with the closed analytical form, where the surface stretching velocity was proportional to the distance from the slot. This problem was later generalized to a power law stretching velocity (Banks, 1983). However, for the power law stretching velocity, the solution was not exact any more. The Crane (1970) problem with suction/injection at the wall was investigated by Gupta and Gupta (1977). Recently, the axisymmetric stretching surface problem was extended to a stretchable disk with both disk stretching and rotation by Fang (2007).

Fang and Zhang (2008) presented an exact solution for the steady state NS equations in cylindrical polar coordinates by a similarity transformation technique. The solution involves the flow between two stretchable infinite disks with accelerated stretching velocity. The transition effect of the boundary layer flow due to a suddenly imposed magnetic field over a viscous flow past a stretching sheet and due to sudden withdrawal of the magnetic field over a viscous flow past a stretching sheet under a magnetic field was analyzed by Kumaran *et al.* (2010). Non dimensionalised equations were solved numerically using the implicit finite difference method of Crank Nicholson type. Ezzat *et al.* (2004) considered perfectly electrically conducting fluid past a non isothermal stretching sheet in the presence of a transverse magnetic field acting perpendicularly to the direction of motion of the fluid. Attia (2007) analyzed the steady MHD laminar three dimensional stagnation point flow of a viscous fluid impinging on a permeable stretching surface with heat generation or absorption. The theoretical analysis of the laminar boundary layer flow and heat transfer of power law non-Newtonian fluids over a stretching sheet was considered by Xu and Liao (2009). Takhar *et al.* (2000) analyzed the flow and mass transfer characteristics of a viscous electrically conducting fluid on a continuously stretching surface having non-zero slot velocity. The implicit finite difference scheme was used to solve the governing partial differential equations. A numerical study of the two dimensional boundary layer stagnation point flow over a stretching sheet in the case of injection/suction through porous medium with heat transfer was considered by Layek *et al.* (2007).

Hayat *et al.* (2009) analyzed the steady two dimensional MHD stagnation point flow of an upper convected Maxwell fluid over the stretching surface. The governing nonlinear partial differential equations were reduced to ordinary ones using the similarity transformation. The homotopy analysis method (HAM) was used to solve these equations. The numerical study of a steady laminar viscous boundary layer flow of an electrically conducting fluid over a heated stretching sheet in the presence of a uniform transverse magnetic field was analyzed by Pantokratoras (2006). Kumaran *et al.* (2009) studied the problem of an MHD boundary layer flow of an electrically conducting fluid over a stretching and permeable sheet with injection/suction through the sheet. The study of a steady two dimensional stagnation point flow of a micropolar fluid over a stretching sheet when the sheet was stretched in its own plane and the stretching velocity was proportional to the distance from the stagnation point was examined by Nazar *et al.* (2004). The resulting coupled equations of nonlinear ordinary differential equations were solved numerically. Desseaux and Kelson (2000) considered a boundary layer flow of a micropolar fluid driven by a porous stretching sheet. A similarity solution was defined, and numerical solutions were obtained using Runge Kutta and quasilinearisation schemes. The analysis of the boundary layer flow of a micropolar fluid on a fixed or continuously moving permeable surface

was presented by Ishak *et al.* (2007). They considered both parallel and reverse moving surfaces to the free stream. The nonlinear ordinary differential equations were solved numerically.

The purpose of the present work is to present a comprehensive parametric study of an MHD flow and heat transfer of a steady incompressible viscous electrically conducting micropolar fluid over a stretching disk in the presence of a uniform magnetic field. A numerical solution is obtained for governing momentum, angular momentum and energy equations using an algorithm based on the finite difference approximation.

2. Problem formulation

Consider an axisymmetric laminar incompressible flow of an electrically conducting micropolar fluid over a stretchable disk. A uniform transverse magnetic field \mathbf{B}_0 is applied at the disk. The governing equations of motion for the MHD laminar viscous flow of a micropolar fluid introduced by Eringen (1964, 1966) are:

— continuity equation

$$\frac{\partial \rho}{\partial t} + (\nabla \cdot \rho \mathbf{V}) = 0 \quad (2.1)$$

— momentum equation

$$(\lambda + 2\mu + \kappa)\nabla(\nabla \cdot \mathbf{V}) + \kappa\nabla \times \mathbf{v} - \nabla p - (\mu + \kappa)[\nabla(\nabla \cdot \mathbf{V}) - \nabla^2 \mathbf{V}] + \mathbf{J} \times \mathbf{B} = \rho \dot{\mathbf{V}} \quad (2.2)$$

— angular momentum equation

$$(\alpha + \beta + \gamma)\nabla(\nabla \cdot \mathbf{v}) - \gamma[\nabla(\nabla \cdot \mathbf{v}) - \nabla^2 \mathbf{v}] + \kappa\nabla \times \mathbf{V} - 2\kappa\mathbf{v} + \rho \mathbf{l} = \rho j \dot{\mathbf{v}} \quad (2.3)$$

— Gauss's law for magnetism

$$\nabla \cdot \mathbf{B} = 0 \quad (2.4)$$

— Ampere's law

$$\nabla \times \mathbf{B} = \mu_m \mathbf{J} \quad (2.5)$$

— Faraday's law of induction

$$\nabla \times \mathbf{E} = \mathbf{0} \quad (2.6)$$

— Ohm's law

$$\mathbf{J} = \sigma_e(\mathbf{E} + \mathbf{V} \times \mathbf{B}) \quad (2.7)$$

where \mathbf{V} is the fluid velocity vector, \mathbf{v} the microrotation, ρ the density, p the pressure, \mathbf{l} the body couple per unit mass, j the microinertia, \mathbf{J} the current density, ∇ the gradient operator, μ_m the magnetic permeability, \mathbf{E} the electric field, \mathbf{B} the total magnetic field so that $\mathbf{B} = \mathbf{B}_0 + \mathbf{b}$, \mathbf{b} the induced magnetic field and σ_e the electrical conductivity of the fluid, λ , μ , α , β , γ , κ the material constants of micropolar fluids (or viscosity coefficients), where the dot signifies material derivatives. From equation (2.4) and (2.5), we see that $\nabla \cdot \mathbf{J} = 0$. The velocity vector \mathbf{V} and the microrotation vector \mathbf{v} are unknown.

The induced magnetic field \mathbf{b} is negligible as compared with the imposed field so that the magnetic Reynolds number is small (Shereliff, 1965). The applied polarization voltage is also assumed to be zero, which implies that the electric field $\mathbf{E} = 0$. The electrical current flowing

in the fluid will give rise to an induced magnetic field which would exist if the fluid was an electrical insulator. We have considered the fluid as electrically conducting, for our problem.

In view of the above assumptions, the electromagnetic body force acting in equation (2.2) has the following linearized form (Rossow, 1958)

$$\mathbf{J} \times \mathbf{B} = \sigma_e [(\mathbf{V} \times \mathbf{B}_0) \times \mathbf{B}_0] = -\sigma_e B_0^2 \mathbf{V} \quad (2.8)$$

A suitable coordinate system for the present problem is a cylindrical polar coordinate system. The components of velocity (u, v, w) and microrotation (v_1, v_2, v_3) along the radial, transverse and axial directions can be written as

$$\begin{aligned} u &= u(r, z) & v &= 0 & w &= w(r, z) \\ v_1 &= 0 & v_2 &= v_2(r, z) & v_3 &= 0 \end{aligned} \quad (2.9)$$

For the problem under consideration, equation (2.8) can be written as

$$\mathbf{J} \times \mathbf{B} = (-\sigma_e B_0^2 u, 0, 0) \quad (2.10)$$

For axisymmetric steady viscous incompressible fluid in the cylindrical polar coordinate system, governing equations of motion (2.1)-(2.3) for the boundary layer approximation, in view of equations (2.8)-(2.10), are reduced to the following dimensionless form:

$$\begin{aligned} \frac{u}{r} + \frac{\partial u}{\partial r} + \sqrt{\frac{\omega}{\nu}} \frac{\partial w}{\partial \eta} &= 0 \\ \rho \left(u \frac{\partial u}{\partial r} + w \sqrt{\frac{\omega}{\nu}} \frac{\partial u}{\partial \eta} \right) &= -\frac{\partial p}{\partial r} - \kappa \sqrt{\frac{\omega}{\nu}} \frac{\partial v_2}{\partial \eta} - \sigma_e B_0^2 u + (\mu + \kappa) \left(\frac{\partial^2 u}{\partial r^2} + \frac{1}{r} \frac{\partial u}{\partial r} + \frac{\omega}{\nu} \frac{\partial^2 u}{\partial \eta^2} - \frac{u}{r^2} \right) \\ \rho j \left(u \frac{\partial v_2}{\partial r} + w \sqrt{\frac{\omega}{\nu}} \frac{\partial v_2}{\partial \eta} \right) &= \kappa \left(\sqrt{\frac{\omega}{\nu}} \frac{\partial u}{\partial \eta} - \frac{\partial w}{\partial r} \right) - 2\kappa v_2 + \gamma \left(\frac{\partial^2 v_2}{\partial r^2} + \frac{1}{r} \frac{\partial v_2}{\partial r} + \frac{\omega}{\nu} \frac{\partial^2 v_2}{\partial \eta^2} - \frac{v_2}{r^2} \right) \end{aligned} \quad (2.11)$$

And the equation for temperature field, neglecting the viscous dissipation, can be written as

$$\rho c_p \left(u \frac{\partial T}{\partial r} + w \sqrt{\frac{\omega}{\nu}} \frac{\partial T}{\partial \eta} \right) - \kappa_0 \left(\frac{\partial^2 T}{\partial r^2} + \frac{1}{r} \frac{\partial T}{\partial r} + \frac{\omega}{\nu} \frac{\partial^2 T}{\partial \eta^2} \right) = 0 \quad (2.12)$$

where T is the temperature, c_p the specific heat at a constant pressure, κ_0 is the thermal conductivity of the fluid, and $\eta = z\sqrt{\omega/\nu}$ is the similarity variable.

Here, the quantity ω is a pseudoangular velocity corresponding to the disk stretching and its unit is 1/s. The boundary conditions over the stretching disk for the velocity field for the present problem are

$$u(r, 0) = r\omega \quad w(r, 0) = 0 \quad u(r, \infty) = 0 \quad (2.13)$$

The no-spin boundary conditions at the boundaries for microrotation are given by

$$(v_1, v_2, v_3) = (0, 0, 0) \quad \text{at} \quad \eta = 0 \quad \text{and} \quad \eta = \infty \quad (2.14)$$

The boundary conditions for the temperature field can be written as

$$T = \begin{cases} T_0 & \text{at} \quad \eta = 0 \\ T_\infty & \text{at} \quad \eta = \infty \end{cases} \quad (2.15)$$

where T_0 is the constant temperature at the disk, and T_∞ is the constant temperature at infinity (with $T_0 > T_\infty$).

In order to obtain the velocity, microrotation and temperature fields for the present problem, we have to solve equations (2.11) and (2.12) subject to the boundary conditions given in equations (2.13) and (2.14). For this purpose, we use the following similarity transformation

$$\begin{aligned} u &= -\frac{r\omega H'(\eta)}{2} & w &= \sqrt{\omega\nu}H(\eta) & p &= \rho\omega\nu P(\eta) \\ v_2 &= \sqrt{\frac{\omega}{\nu}}r\omega g(\eta) & \theta(\eta) &= \frac{T - T_\infty}{T_0 - T_\infty} \end{aligned} \quad (2.16)$$

Using equations (2.16)_{1,2}, we see that continuity equation (2.11)₁ is identically satisfied, and hence velocity components represent a possible fluid motion.

Now by using equations (2.16)_{1,2,3} in momentum equation (2.11)₂, we get

$$\frac{(H')^2}{2} - HH'' + 2c_1g' + (1 + c_1)H''' - M^2H' = 0 \quad (2.17)$$

where

$$c_1 = \frac{\kappa}{\mu} \quad M^2 = \frac{\sigma_e B_0^2}{\rho\omega}$$

are the vortex viscosity parameter and the magnetic parameter, respectively. M is also known as Hartmann number.

Using equations (2.16)₁₋₄ in the angular momentum equation (2.11)₃, we get

$$c_2g'' - c_1\left(\frac{H''}{2} + 2g\right) - c_3\left(Hg' - \frac{H'}{2}g\right) = 0 \quad (2.18)$$

where

$$c_2 = \frac{\gamma\omega}{\nu\mu} \quad c_3 = \frac{\rho\omega j}{\mu}$$

are the spin gradient viscosity parameter and the microinertia density parameter, respectively.

Energy equation (2.12), in view of equations (2.16)_{1,2} and (2.16)₅, takes the form

$$\theta'' - \text{Pr}H\theta' = 0 \quad (2.19)$$

where $\text{Pr} = \mu c_p / \kappa_0$ is the Prandtl number.

Boundary conditions (2.13)-(2.15) in view of transformation equations (2.16) in dimensionless form can be written as

$$\begin{aligned} H(0) &= 0 & H'(0) &= -2 & H'(\infty) &= 0 \\ g(0) &= 0 & g'(\infty) &= 0 & \theta(0) &= 1 & \theta(\infty) &= 0 \end{aligned} \quad (2.20)$$

The quantities of physical interest, the shear and couple stresses on the disk are defined respectively as

$$\begin{aligned} \tau_\omega &= -(\mu + \kappa) \frac{\partial u}{\partial z} \Big|_{z=0} = \mu(1 + c_1)r\omega \sqrt{\frac{\omega}{\nu}} \left(\frac{H''}{2}\right) \Big|_{\eta=0} \\ m_\omega &= -\gamma \frac{\partial v}{\partial z} \Big|_{z=0} = -\gamma r\omega \frac{\omega}{\nu} g' \Big|_{\eta=0} \end{aligned} \quad (2.21)$$

We have to solve the system of equations (2.17), (2.18) and (2.19) subject to the boundary conditions given in equation (2.20).

3. Numerical solution

Governing ordinary differential equations (2.17), (2.18) and (2.19) being highly nonlinear are difficult to solve analytically. We seek for a numerical solution to these equations subject to boundary conditions (2.20) using a finite difference scheme. The order of governing equations (2.17) and (2.18) can be reduced by one as done by Chamkha and Issa (2000), Ashraf and Ashraf (2011) and Ashraf and Bashir (2011), by substituting

$$q = H' = \frac{dH}{d\eta} \quad (3.1)$$

Equations (2.17) and (2.18) in view of equation (3.1) can be written as

$$\begin{aligned} \frac{q^2}{2} - Hq' + 2c_1g' + (1 + c_1)q'' - M^2q &= 0 \\ c_2g'' - c_1\left(\frac{q'}{2} + 2g\right) - c_3\left(Hg' - \frac{q}{2}g\right) &= 0 \end{aligned} \quad (3.2)$$

Boundary conditions (2.20) are reduced as

$$\begin{aligned} H(0) = 0 & \quad q(0) = -2 & \quad q(\infty) = 0 \\ g(0) = 0 & \quad g'(\infty) = 0 & \quad \theta(0) = 1 & \quad \theta(\infty) = 0 \end{aligned} \quad (3.3)$$

For the numerical solution to the above boundary value problem, consisting of equations (3.2) and (2.19), we discretize the domain $[0, \infty)$ uniformly with a step size h . Simpson's rule (Gerald, 1974) with the formula given in Milne (1953) is applied to integrate equation (3.1). The central difference approximations are used to discretize equations (2.19) and (3.2) at a typical grid point $\eta = \eta_n$ of the interval $[0, \infty)$.

The Successive Over Relaxation (SOR) method is used to solve iteratively the obtained system of algebraic equations subject to the associated boundary conditions given in equation (3.3). The solution procedure, which is mainly based on the algorithm described in Syed *et al.* (1997) is used to accelerate the iterative procedure and to improve the accuracy of the solution.

The iterative procedure is stopped if the following criteria is satisfied for four consecutive iterations

$$\max\left(\|q^{(i+1)} - q^{(i)}\|_2, \|g^{(i+1)} - g^{(i)}\|_2, \|H^{(i+1)} - H^{(i)}\|_2, \|\theta^{(i+1)} - \theta^{(i)}\|_2\right) < TOL_{iter} \quad (3.4)$$

Here TOL_{iter} is the prescribed error tolerance, and we have taken at least 10^{-12} for it during our calculations, for the execution of computer programme in Fortran 90. The higher order accuracy of the approximations to the exact solutions is obtained by the use of Richardson's extrapolation. This process is carried out using any extrapolation scheme (Deuffhaard, 1983).

4. Results and discussion

The present study is focused on the numerical investigation of the flow and heat transfer characteristics associated with the steady laminar incompressible viscous flow of an electrically conducting micropolar fluid over the stretchable disk in the presence of a uniform magnetic field. In this Section, a comprehensive numerical study of our findings in tabular and graphical forms together with the discussion and their interpretation is presented. To develop better understanding of the influences of the micropolar structure of electrically conducting fluids on the flow and thermal characteristics in the case of a stretchable disk, we have presented shear and couple stresses at the disk and the velocity, microrotation and temperature fields over the disk

for a range of values of the micropolar parameters (vortex viscosity parameter c_1 , spin gradient viscosity parameter c_2 , microinertia density parameter c_3 , magnetic parameter M , and the Prandtl number Pr).

The results are computed for three grid sizes h , $h/2$ and $h/4$ for the stability of our numerical scheme and then extrapolated on the finer grid using Richardson's extrapolation to obtain more accuracy. A comparison of the numerical values of the axial velocity $H(\eta)$ for the three grid sizes and their extrapolated values is given in Table 1. Excellent comparison validates our computational technique.

Table 1. Comparison of dimensionless axial velocity $H(\eta)$ on three grid sizes and extrapolated values for $M = 2$, $c_1 = 2$, $c_2 = 0.4$, $c_3 = 0.5$ and $Pr = 0.7$

η	$H(\eta)$			
	$h = 0.08$	$h = 0.04$	$h = 0.02$	Extrapolated value
0	0	0	0	0
0.8	-0.965176	-0.964779	-0.964680	-0.964647
1.6	-1.235644	-1.235008	-1.234849	-1.234795
2.4	-1.318906	-1.302135	-1.301970	-1.301915
3.2	-1.322735	-1.318259	-1.318097	-1.318043
4.0	-1.323643	-1.322097	-1.321937	-1.321884
4.8	-1.323858	-1.323008	-1.322849	-1.322796
5.6	-1.323909	-1.323225	-1.323066	-1.323012
6.4	-1.323920	-1.323276	-1.323117	-1.323064
7.2	-1.331510	-1.323287	-1.323117	-1.323075
8.0	-1.323922	-1.323289	-1.323130	-1.323077

For the upper boundary, η_∞ depends on the parameters used. We have adjusted η_∞ in such a way that the profiles become compatible with the asymptotic boundary condition (Pantokratoras, 2009).

Four cases for the values of micropolar parameters c_1 , c_2 and c_3 for the problem under consideration are given in Table 2. The shear and couple stresses and heat transfer rate for the four cases is presented in Table 3. The case 1 ($c_1 = c_2 = c_3 = 0$) stands for Newtonian fluids. The remaining three are for micropolar fluids. It may be noted that micropolar fluids reduce shear stresses as compared to Newtonian fluids. This is due to the reason that micropolar fluids offer a great resistance because of dynamic viscosity and vortex viscosity to the fluid motion as compared to Newtonian fluids.

Table 2. Four cases of micropolar parameters c_1 , c_2 and c_3 discussed

Case No.	c_1	c_2	c_3
1*	0	0	0
2	2	0.2	0.3
3	4	0.4	0.5
4	6	0.6	0.7

* Newtonian

The heat transfer rate $-\theta'(0)$ and couple stresses increase by increasing the values of micropolar parameters c_1 , c_2 and c_3 . The influence of imposition of the external magnetic field on the shear and couple stresses, and the heat transfer rate at the disk is given in Table 4. The applied magnetic field enhances the values of shear stresses, magnitude of couple stresses and

Table 3. Shear and couple stresses, and heat transfer rate over the disk for $M = 2$, $Pr = 0.7$ and for various values of c_1 , c_2 and c_3

Case No.	$H''(0)$	$-g'(0)$	$-\theta'(0)$
1	4.62085	0	0.53752
2	2.41773	2.32706	0.62980
3	1.80029	1.90932	0.69095
4	1.48693	1.66545	0.72756

the heat transfer rate for fixed values of micropolar parameters c_1 , c_2 and c_3 as well as the Prandtl number Pr . The effect of Pr on the heat transfer rate at the disk is given in Table 5. The heat loss increases by increasing the values of the Prandtl number Pr as shown in Table 5. The shear and couple stresses remain unaffected by the variation of Pr .

Table 4. Shear and couple stresses, and values of heat transfer rate over the disk for $c_1 = 3$, $c_2 = 0.1$, $c_3 = 0.2$, $Pr = 0.7$ and for various values of M

M	$H''(0)$	$-g'(0)$	$-\theta'(0)$
0	0.98820	2.19514	0.78550
1	1.29915	2.77224	0.74247
2	1.98111	3.93447	0.65388
3	2.79668	5.16728	0.57386
4	3.67174	6.33861	0.53123
5	4.58056	7.42231	0.53121

Table 5. Values of the heat transfer rate over the disk for $M = 2$, $c_1 = 4$, $c_2 = 0.4$, $c_3 = 0.5$ and for various values of Pr

Pr	$-\theta'(0)$
0.5	0.54422
1.0	0.87874
2.0	1.35695
3.0	1.72319
4.0	2.03143
5.0	2.30279
6.0	2.54809

Now we give the graphical interpretation of velocity, microrotation and thermal fields across the disk.

Figures 1-4 illustrate the influence of micropolar parameters c_1 , c_2 and c_3 on the velocity, microrotation, and temperature fields. The axial velocity profiles $H(\eta)$ decrease for increasing the values of c_1 , c_2 and c_3 as shown in Fig. 1. The magnitude of radial velocity $-H'(\eta)$ and velocity boundary layer thickness increase by increasing the values of micropolar parameters c_1 , c_2 and c_3 as shown in Fig. 2. Figure 3 presents the effect of micropolar parameters c_1 , c_2 and c_3 on the microrotation for $M = 2$ and $Pr = 0.7$. Case 1 corresponds to Newtonian fluids and, therefore, there is no microrotation in this case. The other three cases show that the micropolar parameters have significant influence on the microrotation. The magnitude of microrotation $g(\eta)$ increases by increasing the values of c_1 , c_2 and c_3 . The microrotation profiles increase far from the boundary and decrease near the boundary. The temperature profiles for four cases of micropolar parameters decrease by increasing the values of c_1 , c_2 and c_3 as shown in Fig. 4. The thermal boundary layer thickness decreases by increasing the values of micropolar parameters c_1 , c_2 and c_3 .

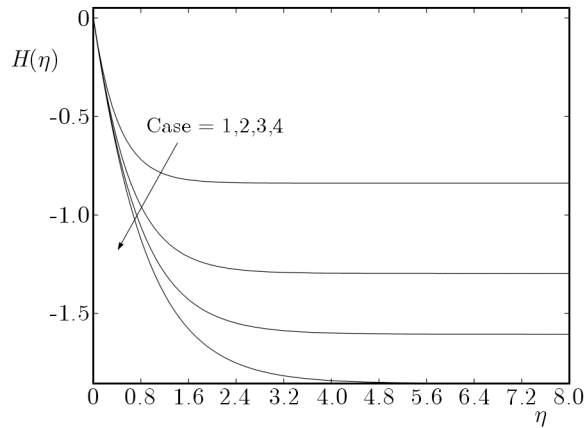


Fig. 1. Variation of dimensionless axial velocity $H(\eta)$ for $M = 2$, $Pr = 0.7$ and for various values of micropolar parameters c_1 , c_2 and c_3

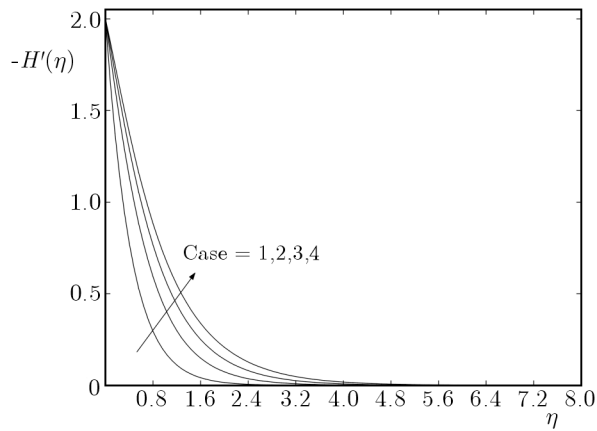


Fig. 2. Variation of dimensionless radial velocity $-H'(\eta)$ for $M = 2$, $Pr = 0.7$ and for various values of micropolar parameters c_1 , c_2 and c_3

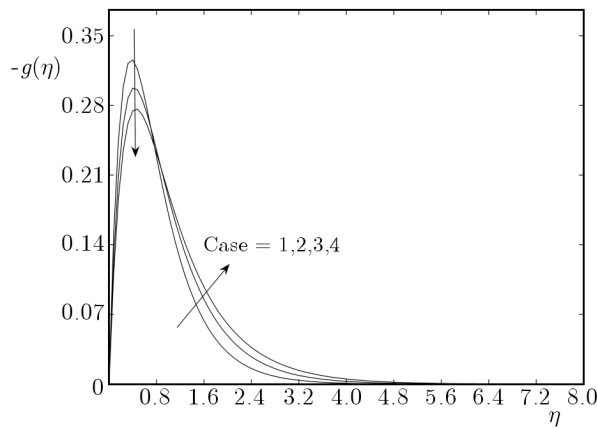


Fig. 3. Variation of microrotation profile $-g(\eta)$ for $M = 2$, $Pr = 0.7$ and for various values of micropolar parameters c_1 , c_2 and c_3

Figure 5 shows that the magnitude of axial velocity decreases as the value of increases. Figure 6 presents the influence of the applied magnetic field for fixed values of micropolar parameters c_1 , c_2 , c_3 and the Prandtl number Pr on radial velocity. The results indicate that the magnitude of radial velocity decreases with increasing values of M . Furthermore, the velocity boundary layer becomes thinner by increasing the values of M . The reverse flow caused due to the stretching of the disk can be controlled/stopped by applying a strong magnetic field.

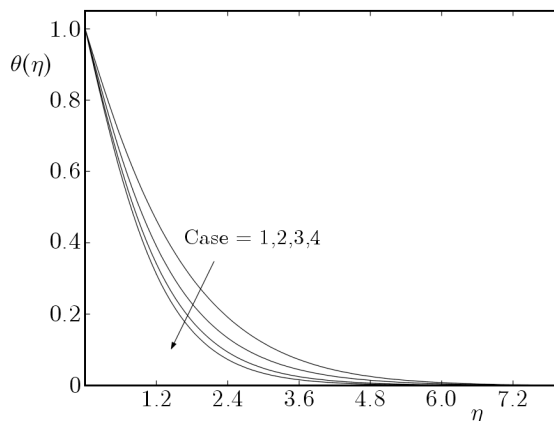


Fig. 4. Variation of temperature profile $\theta(\eta)$ for $M = 2$, $Pr = 0.7$ and for various values of micropolar parameters c_1 , c_2 and c_3

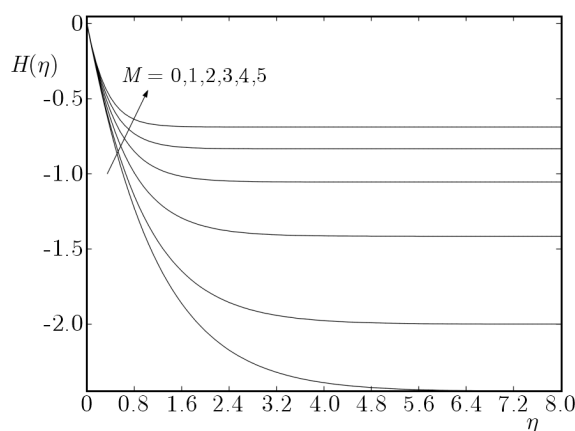


Fig. 5. Variation of dimensionless axial velocity $H(\eta)$ for $c_1 = 3$, $c_2 = 0.1$, $c_3 = 0.2$, $Pr = 0.7$ and for various values of M

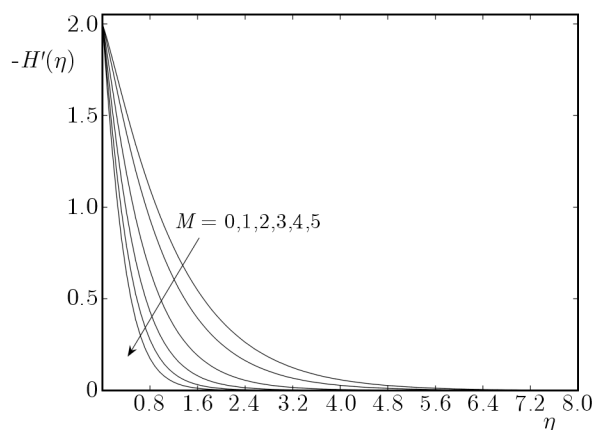


Fig. 6. Variation of dimensionless radial velocity $-H'(\eta)$ for $c_1 = 3$, $c_2 = 0.1$, $c_3 = 0.2$, $Pr = 0.7$ and for various values of M

Figure 7 illustrates the effect of the magnetic field on the microrotation for fixed values of the micropolar parameters c_1 , c_2 and c_3 as well as the Prandtl number Pr . The microrotation profiles decrease far from the boundary and a reverse effect is found near the boundary. The microrotation profiles decrease due to the damping effect of the magnetic field which shows that the intensity of the applied magnetic field can be used to decrease the angular rotation especially in suspension flows, arising in lubrication problems. The effect of the magnetic field on the

temperature distribution for fixed values of c_1, c_2, c_3 and Pr is shown in Fig. 8. An increase in the temperature profiles is observed with an increase in the values of M . The thermal boundary layer increases by increasing the values of M .

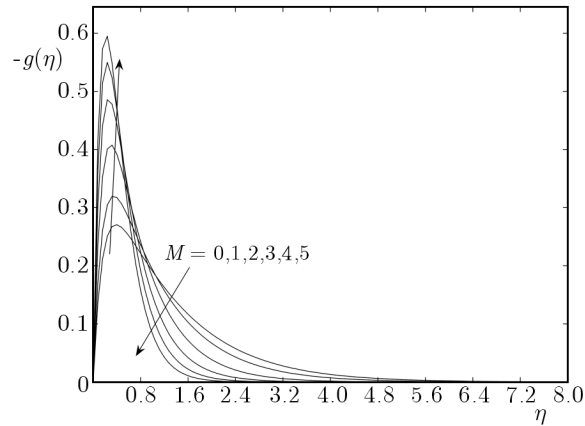


Fig. 7. Variation of microrotation profile $-g(\eta)$ for $c_1 = 3, c_2 = 0.1, c_3 = 0.2, Pr = 0.7$ and for various values of M

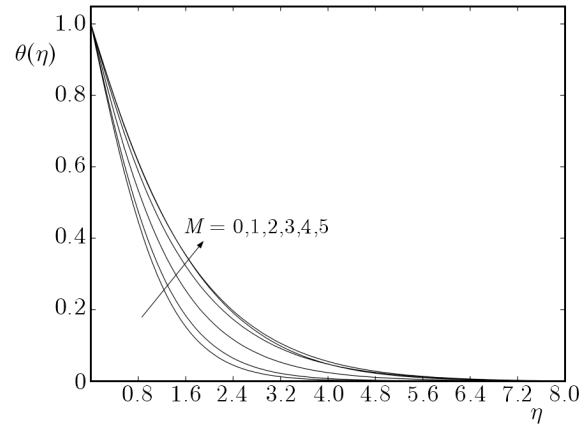


Fig. 8. Variation of temperature profile $\theta(\eta)$ for $c_1 = 3, c_2 = 0.1, c_3 = 0.2, Pr = 0.7$ and for various values of M

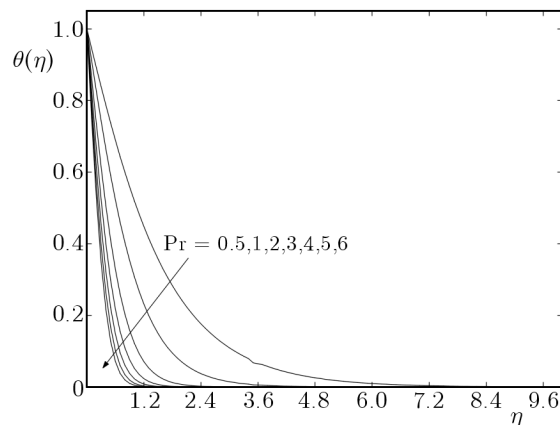


Fig. 9. Variation of temperature profile $\theta(\eta)$ for $c_1 = 4, c_2 = 0.4, c_3 = 0.5, M = 2$ and for various values of Pr

Figure 9 illustrates the variation of dimensionless temperature $\theta(\eta)$ for selected values of the Prandtl number Pr . An increase in the values of Pr results in the fall of temperature profiles and thinning of the thermal boundary layer.

5. Conclusions

A numerical study of the MHD flow and heat transfer of an electrically conducting micropolar fluid in the presence of the applied magnetic field over a stretchable disk is presented to describe the effects of some governing parameters. Numerical solutions to the transformed self similar governing equations and the associated boundary conditions have been obtained using a finite difference discretization method. The following conclusions have been made.

- Micropolar fluids reduce the shear stresses and enhance couple stresses as compared to Newtonian fluids.
- Velocity boundary layer thickness increases by increasing the value of micropolar parameters.
- The magnetic field enhances the shear stresses and heat transfer rate.
- The velocity boundary layer becomes thinner, while the thermal boundary layer becomes thicker by increasing the values of the magnetic parameter.
- Increasing the Prandtl number decreases the thermal boundary layer thickness.

Acknowledgement

The authors acknowledge the financial support by Higher Education Commission (HEC), Pakistan under the indigenous scholarship programme Batch IV.

References

1. ASHRAF M., ASHRAF M.M., 2011, Stagnation point flow of a micropolar fluid towards a heated surface, *Applied Mathematics and Mechanics(English Edition)*, **32**, 45-54
2. ASHRAF M., BASHIR S., 2011, Numerical simulation of MHD stagnation point flow and heat transfer of a micropolar fluid towards a heated shrinking sheet, *Int. J. Numer. Meth. Fluid*, DOI: 10.1002/flid.2564
3. ATTIA H.A., 2007, Axissymmetric stagnation point flow towards a stretching surface in the presence of a uniform magnetic field with heat generation, *Tamkang Journal of Science and Engineering*, **10**, 11-16
4. BANKS W.H., 1983, Similarity solutions of the boundary layer equations for a stretching wall, *J. Mech. Theor. Appl.*, **2**, 375-392
5. CHAMKHA A.J., ISSA C., 2010, Effects of heat generation/absorption and thermophoresis on hydromagnetic flow with heat and mass transfer over a flat surface, *Int. J. Numer. Methods Heat Fluid Flow*, **10**, 432-449
6. CRANE L.J., 1970, Flow past a stretching plate, *Z. Angew. Math. Phys. (ZAMP)*, **21**, 645-647
7. DESSEAUX A., KELSON N.A., 2000, Flow of a micropolar fluid bounded by a stretching sheet, *Anziam*, **42**, C536-C560
8. DEUFLHAARD P. 1983, *Order and step size control in extrapolation methods*, *Numerische Mathematic*, **41**, 399-422
9. ERINGEN A.C., 1964, *Simple microfluids*, *International Journal of Engineering Science*, **2**, 205-217
10. ERINGEN A.C., 1966, *Theory of micropolar fluids*, *Journal of Mathematics and Mechanics*, **16**, 1-18
11. EZZAT M., ZAKARIA M., MOURSY M., 2004, Magnetohydrodynamic boundary layer flow past a stretching plate and heat transfer, *Journal of Applied Mathematics*, **1**, 9-21

12. FANG T., 2007, Flow over a stretchable disk, *Phys. Fluids*, **19**, 128105
13. FANG T., ZHANG J., 2008, Flow between two stretchable disks – an exact solution of the Navier Stokes equations, *International Communications in Heat and Mass Transfer*, **35**, 892-895
14. GERALD C.F., 1974, *Applied Numerical Analysis*, Addison Wesley Publishing Company Reading Massachusetts
15. GUPTA P.S., GUPTA A.S., 1977, Heat and mass transfer on a stretching sheet with suction or blowing, *Can. J. Chem. Eng.*, **55**, 744-746
16. HAYAT T., ABBAS Z., SAJID M., 2009, MHD stagnation point flow of an upper convected Maxwell fluid over a stretching sheet, *Chaos Solitons and Fractals*, **39**, 840-848
17. ISHAK A., NAZAR R., POP I., 2008, Magnetohydrodynamic (MHD) flow of a micropolar fluid towards a stagnation point on a vertical surface, *Computers and Mathematics with Applications*, **56**, 3188-3194
18. KUMARAN V., BANERJEE A.K., KUMAR A.V., VAJRARELU K., 2009, MHD flow past a stretching permeable sheet, *Applied Mathematics and Computation*, **210**, 26-32
19. KUMARAN V., KUMAR A., POP I., 2010, Transition of MHD boundary layer flow past a stretching sheet, *Commun Nonlinear Sci. Numer. Simulat.*, **15**, 300-311
20. LAYEK G.C., MUKHOPADHYAY S., SAMAD S.A., 2007, Heat and mass transfer analysis for boundary layer stagnation point flow towards a heated porous stretching sheet with heat absorption/generation and suction/blowing, *International Communications in Heat and Mass Transfer*, **34**, 347-356
21. MILNE W.E., 1953, *Numerical Solutions of Different Equations*, John Willey and Sons Inc., New York
22. NAZAR R., AMIN N., FILIP D., POP I., 2004, Stagnation point flow of a micropolar fluid towards a stretching sheet, *International Journal of Non-Linear Mechanics*, **39**, 1227-1235
23. PANTOKRATORAS A., 2006, Study of MHD boundary layer flow over a heated stretching sheet with variable viscosity, *International Journal of Heat and Mass Transfer*, **51**, 104-110
24. PANTOKRATORAS A., 2009, A common error made in investigation of boundary layer flows, *Applied Mathematical Modelling*, **33**, 413-422
25. ROSSOW V.J., 1958, On flow of electrically conducting fluids over a flat plate in the presence of a transverse magnetic field, *Tech. Report 1358 NASA*
26. SAKIADIS B.C., 1961, Boundary layer behavior on continuous solid surface: II. Boundary layer on a continuous flat surface, *AIChE Journal*, **7**, 221-225
27. SHERELIFF J.A., 1965, *A Textbook of Magnetohydrodynamics*, Pergoman Press
28. SYED K.S., TUPHOLME G.E., WOOD A.S., 1997, Iterative solution of fluid flow in finned tubes, [In:] *Proceedings of the 10th International Conference on Numerical Methods in Laminar and Turbulent Flow*, C. Taylor and J.T. Cross (Eds.), 429-440
29. TAKHAR H.S., CHAMKA A.J., NATH G., 2000, Flow and mass transfer on a stretching sheet with a magnetic field and chemically reactive species, *International Journal of Engineering Science*, **38**, 1303-1314
30. XU H., LIAO S.-J., 2009, Laminar flow and heat transfer in the boundary layer of non-Newtonian fluids over a stretching flat sheet, *Computers and Mathematics with Applications*, **57**, 1425-1431

Przepływ magneto hydrodynamiczny oraz przewodzenie ciepła w cieczy mikropolarnej opływającej rozciągliwy dysk

Streszczenie

W pracy zaprezentowano wyniki badań numerycznych nad osiowo-symetrycznym, laminarnym i ustalonym opływem elektrycznie przewodzącej cieczy mikropolarnej wokół rozciągliwego dysku przy jednoczesnym oświetleniu cieczy polem magnetycznym. Nieliniowe równanie ruchu opływu sprowadzono do postaci bezwymiarowej za pomocą funkcji podobieństwa von Karmana. Do rozwiązania uproszczonych, sprzężonych i nieliniowych równań różniczkowych zwyczajnych z towarzyszącymi warunkami brzegowymi użyto algorytmu opartego na metodzie różnic skończonych. Przedyskutowano wpływ parametrów mikropolarności, wartości pola magnetycznego oraz liczby Prandtla na rozkład prędkości i temperatury cieczy. Według badań, tempo przepływu ciepła na powierzchni dysku wzrasta z rosnącymi wartościami parametrów mikropolarności. Dodatkowo, obecność pola magnetycznego powiększa naprężenia ścinające i momentowe. Wartość naprężeń ścinających jest mimo to mniejsza dla cieczy mikropolarnej niż dla newtonowskiej, co może być korzystne w monitorowaniu przepływu i transferu ciepła podczas procesu obróbki polimerów.

Manuscript received December 13, 2011; accepted for print March 1, 2012